Weierstraß-Institut

für Angewandte Analysis und Stochastik

Leibniz-Institut im Forschungsverbund Berlin e. V.

Preprint ISSN 0946 – 8633

Multistability of twisted states in non-locally coupled Kuramoto-type models

Taras Girnyk[1], Martin Hasler[2], Yuriy Maistrenko[3]

submitted: February 13, 2012

[1] Weierstrass Institute
Mohrenstr. 39 10117 Berlin, Germany
E-Mail: taras.girnyk@wias-berlin.de

[2] Laboratory of Nonlinear Systems
School of Computer and Communication Sciences
Ecole Polytechnique Federale de Lausanne
CH 1015 Lausanne, Switzerland
E-Mail: martin.hasler@epfl.ch

[3] Institute of Mathematics, National Academy of Sciences of Ukraine,
Tereshchenkivska St. 3, 01601 Kyiv, Ukraine
E-Mail: y.maistrenko@biomed.kiev.ua

No. 1685

Berlin 2012

2010 *Mathematics Subject Classification.* Primary 37C75.

2010 *Physics and Astronomy Classification Scheme.* 05.45.Xt, 02.60.-x.

Key words and phrases. Chaos, Nonlinear dynamical systems, Numerical analysis, Oscillators.

Edited by
Weierstraß-Institut für Angewandte Analysis und Stochastik (WIAS)
Leibniz-Institut im Forschungsverbund Berlin e. V.
Mohrenstraße 39
10117 Berlin
Germany

Fax: +49 30 2044975
E-Mail: preprint@wias-berlin.de
World Wide Web: http://www.wias-berlin.de/

Abstract

A ring of N identical phase oscillators with interactions between L-nearest neighbors is considered, where L ranges from 1 (local coupling) to $N/2$ (global coupling). The coupling function is a simple sinusoid, as in the Kuramoto model, but with a minus sign which has a profound influence on its behavior. Without limitation of the generality the frequency of the free-running oscillators can be set to zero. The resulting system is of gradient type and therefore all its solutions converge to an equilibrium point. All so-called q-twisted states, where the phase difference between neighboring oscillators on the ring is $2\pi q/N$ are equilibrium points, where q is an integer. Their stability in the limit $N \to \infty$ is discussed along the line of [Wiley, Strogatz, and Girvan(2006)]. In addition we prove that when a twisted state is asymptotically stable for the infinite system, it is also asymptotically stable for sufficiently large N. Note that for smaller N, the same q-twisted states may become unstable and other q-twisted states may become stable. Finally, the existence of additional equilibrium states, called here multi-twisted states, is shown by numerical simulation. The phase difference between neighboring oscillators is approximately $2\pi q/N$ in one sector of the ring, $-2\pi q/N$ in another sector, and it has intermediate values between the two sectors. Our numerical investigation suggests that the number of different stable multi-twisted states grows exponentially as $N \to \infty$. It is possible to interpret the equilibrium points of the coupled phase oscillator network as trajectories of a discrete-time translational dynamical system where the space-variable (position on the ring) plays the role of time. The q-twisted states are then fixed points and the multi-twisted states are periodic solutions of period N that are close to a heteroclinic cycle. Due to the apparently exponentially fast growing number of such stable periodic solutions, the system shows spatial chaos as $N \to \infty$.

Oscillators are important dynamical systems. They are ubiquitous in biology and they are used in many man-made devices. Networks of coupled oscillators are also frequently found in biology and they start being used in technology [Degallier and Ijspeert(2010)]. A fundamental question is whether such oscillators synchronize, i.e. whether or not they oscillate at the same frequency.

The simplest model for an oscillator is a pair of first order ordinary differential equations, with suitable parameters to ensure oscillatory behavior. A number of them can be aggregated into a network, usually by coupling through one of their dynamical (state-) variables. If the coupling is weak, then the orbit of each oscillator is perturbed only very slightly, whereas its phase is very sensitive to the coupling. Therefore, under weak coupling, the dynamical behavior of the network of oscillators is reproduced very well by a system of differential equations for the phases only, one per oscillator, which is a substantial simplification.

The phase of each oscillator, when decoupled from the other oscillators, increases linearly, i.e. its angular frequency is constant. After averaging, the coupling between two oscillators usually obeys the form of a 2π-periodic function of their phase differences. The best known network of phase oscillators is the so-called Kuramoto model where the oscillators are coupled through the sinus of the phase differences in a homogeneous all-to-all fashion. The network studied in

this paper differs from the Kuramoto model in three aspects: The coupling is not all-to-all, the coupling function has the opposite sign and all oscillators have the same free-running frequency.

The N oscillators in our network are disposed on a ring and interaction takes place among the L-nearest neighbor oscillators on the ring. The interaction function between two oscillators is proportional to the sinus of the phase difference, with a sign that makes the interaction repulsive for small phase differences. Note that in the Kuramoto model, the interaction for small phase differences is attractive. Finally, the free-running angular frequencies are all the same, say ω, whereas in the Kuramoto model they are generally different, but concentrated around a mean frequency. If they were also identical in the Kuramoto model, all oscillators would synchronize and oscillate together stably with angular frequency ω and identical phases.

Our system has N dynamical regimes where all oscillators have identical angular frequency and constant phase differences $2\pi q/N$ between neighbors on the ring, the so-called q-twisted states. The sign of the interaction in the system does not matter in this respect. It makes a big difference, however, when the stability of the q-twisted states are considered. For attractive coupling, this question is addressed in [Wiley, Strogatz, and Girvan(2006)]. There, a rigorous stability analysis of the q-twisted states in the limit as $N \to \infty$ is carried out. We have applied the same type of analysis in our case of repulsive coupling. As a result, we obtain an interval for qr where the infinite N stability conditions are satisfied, and this implies that for each value of qr in this interval we can find a sufficiently large N and an $L \approx (rN-1)/2$, such that the q-twisted state in this finite size system is stable. This gives a whole family of stable q-twisted states. Even though, when N is finite, we can only guarantee their stability for large enough N, numerical simulations show that they are also stable even for moderate values of N. In addition to this principal family of stable q-twisted states there are small islands in (r,q)-parameter plane where the infinite N system and therefore also the finite N system for large enough N have stable q-twisted states.

Finally, the existence of additional stable dynamical regimes, where the oscillators also have the common angular frequency, but where the phase differences between neighboring oscillators are not uniform around the ring, is shown by numerical simulations. In fact, in one sector of the ring, the phase differences between neighboring oscillators is approximately $2\pi q/N$, in another sector it is $-2\pi q/N$, and in between it has intermediate values. There is some interesting interpretation of these solutions from the point of view of dynamical systems theory. In particular, our simulations indicate the presence of spatial chaos as $N \to \infty$.

1 Introduction

Starting with the pioneering works of Winfree [Winfree(1967), Winfree(2001)], Kuramoto [Kuramoto(2002), Kuramoto(1984)], and Ermentrout [Kopell and Ermentrout(1990), Ermentrout(1985a), Ermentrout and Kopell(1984)] a novel, rapidly developing branch of nonlinear science has appeared, which deals with the complex collective dynamics of the networks of coupled oscillators. This type of models arises in very different fields ranging from physics and engineering through biology and medicine up to economics and social studies (see [Strogatz(2oo1), Strogatz(1999), Boccaletti(2008)] for more references). Important, rapidly growing applications come from neuroscience, where studying neuronal networks is a crucial task for understanding the functioning of the brain. Another challenging task is the spatial orga-

nization and the dynamics of genetic networks.

In the Kuramoto-type models each oscillator is reducible to a single phase variable, and the coupling between the oscillators depends only on the phase differences between them [Ermentrout(1985b), Strogatz(2oo1), Strogatz(1999), Boccaletti(2008)]. Mathematically, the most tractable is the case of a ring coupling topology, i.e. a one-dimensional chain of oscillators with periodic boundary conditions. If so, one of the main characteristics for the network dynamics becomes the range of coupling. The most comprehensive results concern two extreme cases: either local (nearest-neighbor) coupling, where each oscillator interacts only with its two neighbors [Kopell and Ermentrout(1990), Ermentrout(1985a), Ermentrout and Kopell(1984)] or global (all-to all) coupling [Winfree(1967), Winfree(2001), Kuramoto(2002), Kuramoto(1984), Ermentrout(1985b), Strogatz(2000), Mirollo and Strogatz(1990), Daido(1997), Crawford and Davies(1999), Ott *et al.*(2002)Ott, So, Barreto, and Antonsen]. It should be mentioned that in all-to-all interaction the coupling topology losses its sense: actually, each oscillator is forced by the same mean-field type impact of all others. This fact essentially simplifies the study and allows, in many situations, to propose original analytical approaches to the collective system dynamics [Ott and Antonsen(2008), Watanabe and Strogatz(1993), Pikovsky and Rosenblum(2009)]. On the other hand, the intermediate case, in which the coupling spreads beyond the nearest-neighbors but does not captivate the whole network, is far less studied [Ermentrout(1985a), Kopell, Zhang, and Ermentrout(1990), Kiem *et al.*(2004)Kiem, Ko, Jeong, and Moon]. This looks rather surprising in the light of numerous applications of non-local coupling in different fields. To cite one, neuronal networks in the brain: it is experimentally established that each neuron is connected to about 10% of the other neurons in the specific brain region where it is located [Lefort *et al.*(2009)Lefort, Tomm, Sarria, and Petersen].

Recently, a new interest in non-locally coupled oscillators appeared due to the discovery of the so-called *chimera states* [Kuramoto and Battogtokh(2002), Abrams and Strogatz(2004), Laing(2009), Omelchenko, Wolfrum, and Maistrenko(2010)]. These hybrid spatio-temporal patterns are characterized by co-existence of phase-locked and drifting oscillators. This kind of solutions are unusual for networks of identical oscillators with only local or only global coupling, but they typically arise in the presence of non-local coupling. As it was illustrated in [Wiley, Strogatz, and Girvan(2006)], the essential differences between the globally and non-globally coupled networks are clearly visible already for the simplest case of identical sinusoidal phase oscillators on a ring:

$$\dot{\phi_i} = \omega + \frac{1}{2L+1}\sum_{j=-L}^{L}\sin\left(\phi_{i+j} - \phi_i\right), i = 1, \ldots, N \tag{1}$$

Here each oscillator ϕ_i is coupled with equal strength to its L nearest neighbors on both sides, and therefore collective dynamics can only be determined by the number of oscillators N and by the range of coupling $r = (2L+1)/N$. If $r = 1$ (all-to-all coupling), fully synchronized coherent solutions $\phi_i = \omega t + C$, $i = 1, \ldots, N$, are the only possible attractors for the model. These solutions preserve their stability with decreasing r from 1 to 0, but, in addition new states stabilize one after another in the form of uniformly twisted traveling waves

$$\phi_i = \omega t + \frac{2\pi q i}{N} + C, i = 1, \ldots, N \tag{2}$$

for all $q = 1, \ldots, N-1$. First, when r goes below a critical value (approximately equal 0.68) the solutions with $q = \pm 1$, i.e. a standard splay state, becomes stable; then, at $r \approx 0.34$ the next

two states with $q = \pm 2$ stabilize and so on. Therefore, multistability arises in the non-locally coupled model (1), and it becomes more and more developed with decreasing range of coupling r. We illustrate this in Fig. 1a, where all stable twisted states for the model with $N = 20$ are indicated by solid dots in the parameter plane (L, q). In [Wiley, Strogatz, and Girvan(2006)] a rigorous proof of the stability of the twisted states in the form of (2) is given as $N \to \infty$, and it is postulated (on the basis of numerical simulations) that their stability also extends to the case of not only large, but also moderately large N.

In the present paper, we apply a similar approach to the *repulsive* Kuramoto-like model

$$\dot{\phi}_i = \omega - \frac{1}{2L+1} \sum_{j=-L}^{L} \sin\left(\phi_{i+j} - \phi_i\right), i = 1, \ldots, N \tag{3}$$

i.e. where the sign of the interaction is changed from + to -. In this system, as we found, the repulsive characters of coupling leads to a different and more involved bifurcation structure as a function of the radius of interaction r, which is illustrated in Fig. 1b. For the model (3) we trace changes in the system dynamics depending on the coupling range $r = (2L+1)/N$, and prove stability of the q-twisted states for both finite and infinite N (Ch.s 3 and 4 respectively), as well as their asymptotic equivalence (Appendix). Finally, we detected the existence and stability of so-called *multi-twisted states* each of which is a combination of positive and negative phase differences of the same size between neighboring oscillators on the ring (Ch. 6). This type of rotating waves has not been observed in the attractively coupled model [Wiley, Strogatz, and Girvan(2006)]. On the other hand, they typically arise in the repulsive model (3) at rather small values of the coupling range r, but not in the nearest-neighbor coupling case. If we consider the associated translational dynamical system that maps, for fixed time, at each step the phase difference of neighboring oscillator to the phase difference of the next oscillators on the ring, then the q-twisted states are fixed points and the multi-twisted states exhibit alternations between the clock-wise and anti-clock-wise rotations of the phase approximately by the same amount. Therefore, the multi-twisted states can be interpreted as heteroclinic cycles of the translational dynamical system, where the role of time is played by space variable i. Our numerical simulations indicate that the number of different stable multi-twisted states (periodic orbits, closed to the heteroclinic passes) grows exponentially with N giving rise, therefore, to the phenomenon of spatial chaos [Jensen(1985), Coullet, Elphick, and Repaux(1987), Chow and Mallet-Paret(1995), Nizhnik, Nizhnik, and Hasler(2002), Afraimovich(2005), Fernandez, Luna, and Ugalde(2009)]. Also, we note that the synchronization in a more general array of Kuramoto-like oscillators with repulsive coupling was investigated in [Tsimring *et al.*(2005)Tsimring, Rulkov, Larsen, and Gabbay].

2 Model

We consider a one-dimensional ring of N identical phase oscillators, each coupled with equal strength to its L nearest neighbors on either side (3) where the index i is periodic mod N. Compared to the standard Kuramoto model [Kuramoto(1984), Strogatz(2000)] coupling is not global for $2L < N - 1$. Another peculiarity is the negative sign of the interaction term in Eq. (3). This can be interpreted as repulsive (or inhibitory) coupling, at least when the phase differences are small. Apart from the sign change, it is the same model as considered in [Wiley, Strogatz, and Girvan(2006)], where the interaction is attractive (excitatory). This seems

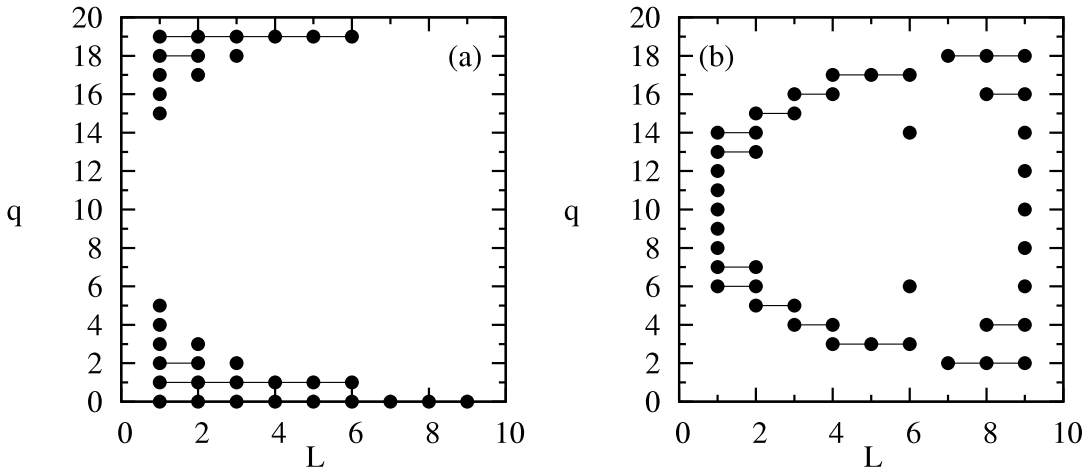

Figure 1: Stability of q-twisted states (2): a) for the attractive Kuramoto-like model (1) b) for the repelling Kuramoto-type model (3) of $N = 20$ oscillators. Solid dots indicate (L,q)-parameter values for the q-twisted states which are stable in the model with L-nearest neighbor coupling. Note that there are many stable q-twisted states in the nearest-neighbor coupling case $L = 1$ (for both attractive and repelling models). It is not surprising that the fully coherent state $(q = 0)$ in attractive model (1) is stable for any L. On the other hand, any even q-twisted state is stable in the repelling model (3) with maximal non-global coupling range $L = 9$.

to be a minor change, but it has a profound influence on the qualitative behavior of the solutions as illustrated in Fig. 1 for the network of $N = 20$ oscillators. Here the horizontal lines represent ßtability intervals"for the q-twisted states (2) for different values of the parameter q as a function of the coupling range L for positive (Fig. 1a) and for negative (Fig. 1b) coupling - i.e. for model (1) and (3) respectively. Let us mention the most striking differences. The coherent solutions $(q = 0)$ are always stable for positive but never stable for negative coupling, which could be expected. Furthermore, the most prominent twisted states with $q = \pm 1$ (also called *splay states*) are stable for a rather long coupling range for positive coupling, but never stable for negative coupling (except for the globally coupled case $L = N - 1/2$), which has come as a surprise for us. Instead, twisted states with $q = \pm 2$ and $q = \pm 3$ appear to be stable for the longest L-interval. Other differences will be discussed later in the paper.

Basically, to study the stability of the q-twisted states we first proceed in the way proposed in [Wiley, Strogatz, and Girvan(2006)]. System (3) can be simplified by the substitution

$$\phi_i \to \phi_i + \omega t, \tag{4}$$

which leads to

$$\dot{\phi}_i = -\frac{1}{2L+1} \sum_{j=-L}^{L} \sin\left(\phi_{i+j} - \phi_i\right), i = 1, \ldots, N. \tag{5}$$

This transforms the q-twisted states from uniformly rotating waves to equilibrium points. As usual, the order parameter is defined as

$$R = \frac{1}{N} \sum_{i=1}^{N} e^{i\phi_i}. \tag{6}$$

System (5) is of gradient type with the potential function

$$F(\phi) = \frac{1}{2L+1} \sum_{i=1}^{N} \sum_{j=-L}^{L} \cos(\phi_{i+j} - \phi_i).$$

Therefore, the only possible asymptotic behavior is the convergence to an equilibrium point.

3 Stability analysis of the twisted states for $N \to \infty$

In this section we will examine stability of the twisted states in the limit when $N \to \infty$. After removing the frequency ω by the substitution (4) the twisted states

$$\phi_i = \frac{2\pi q i}{N},\ i = 1, \ldots, N$$

are equilibrium points of Eq. (5) for any $q = 0, \pm 1, \pm 2, \ldots$. Their stability remains to be investigated. For this purpose, we follow the approach proposed in [Wiley, Strogatz, and Girvan(2006)]. Let us introduce the coupling range $r = (2L+1)/N$ which is supposed to be smaller than 1, and consider the corresponding coupling function

$$G(x) = \begin{cases} \frac{1}{2\pi r},\ |x| \le \pi r \\ 0,\ |x| > \pi r. \end{cases} \tag{7}$$

We can rewrite system (5) as

$$\dot{\phi}_i = -\frac{2\pi}{N} \sum_{j=1}^{N} G\left(\frac{2\pi}{N}(i-j)\right) \sin(\phi_j - \phi_i), i = 1, \ldots, N. \tag{8}$$

In the limit $N \to \infty$ Eq. (8) becomes

$$\frac{\partial \phi}{\partial t} = -\int_0^{2\pi} G(x-y) \sin(\phi(y,t) - \phi(x,t)) dy, \tag{9}$$

where $\phi(x,t)$ is the phase of the oscillator at position $|x|$ (corresponding to $2\pi i/N$ for oscillator number i in the case of finite N) at time t. Note, that $\phi(x,t)$ should be 2π periodic in x. In the limit $N \to \infty$ the twisted states take the form

$$\phi(x,t) = qx \mod 2\pi. \tag{10}$$

They are equilibrium solutions of the integral equation (9) for any integer q. In order to obtain stability conditions for the twisted states, we apply a small perturbation $\eta(x,t)$ that is 2π periodic in x:

$$\phi(x,t) = qx + \eta(x,t) \mod 2\pi. \tag{11}$$

Linearization of (9) around qx yields

$$\frac{\partial \eta}{\partial t} = -\int_0^{2\pi} G(x-y) \cos(q(x-y))[\eta(y,t) - \eta(x,t)] dy, \tag{12}$$

which can be re-written as

$$\frac{\partial \eta}{\partial t} = -\int_0^{2\pi} G(x-y)\cos\left(q(x-y)\right)\eta(y,t)dy + \eta(x,t)\int_0^{2\pi} G(x-y)\cos\left(q(x-y)\right)dy. \quad (13)$$

We can expand this equation into Fourier series. The m-th Fourier component $\tilde{\eta}_m(t)$ satisfies the equation

$$\frac{d\tilde{\eta}_m(t)}{dt} = \left[\frac{\tilde{G}_q + \tilde{G}_{-q}}{2} - \frac{\tilde{G}_{q+m} + \tilde{G}_{m-q}}{2}\right]\tilde{\eta}_m(t), \quad (14)$$

where $\tilde{G}$ denotes the Fourier transform of G. Since G is an even function, i.e. $\tilde{G}_q = \tilde{G}_{-q}$, the equation becomes

$$\frac{d\tilde{\eta}_m(t)}{dt} = \left[\tilde{G}_q - \frac{\tilde{G}_{q+m} + \tilde{G}_{q-m}}{2}\right]\tilde{\eta}_m(t).$$

Therefore, if

$$\tilde{G}_q - \frac{\tilde{G}_{q+m} + \tilde{G}_{q-m}}{2} < 0,\ m = 1, 2, \ldots$$

then the twisted state qx is stable. Note, that for $m = 0$ we get

$$\frac{d\tilde{\eta}_0(t)}{dt} = 0,$$

which corresponds to a simultaneous shift of all phases by the same amount $(\phi_i \to \phi_i + C)$ and therefore $\eta_0(t) = \eta_0(0)$. It is convenient to re-write the system in phase differences in order to get rid of this phase shift and to operate with asymptotically stable equilibrium points. In the case, when $G(x)$ is given by Eq. (7) we obtain

$$\tilde{G}(q) = \frac{\sin \pi q r}{\pi q r}. \quad (15)$$

This leads to the stability criterion

$$s(qr) - \frac{1}{2}[s(qr + mr) + s(qr - mr)] < 0, m = 1, 2, \ldots, \quad (16)$$

where $s(x) = \frac{\sin(\pi x)}{\pi x}$. Note, that now expression in the left-hand side of (16) is an even function with respect to qr. Due to this, it is possible to consider only the case $q > 0$ and therefore both q and $-q$ twisted states are stable or unstable simultaneously.

Let us introduce the new variables $\rho = qr$ and $\mu = mr$, and suppose ρ and μ can take any positive real value. Then, the stability condition becomes as follows: the twisted state given by $\rho = qr$ is (linearly) stable if

$$f(\rho, \mu) := s(\rho) - \frac{1}{2}[s(\rho + \mu) + s(\rho - \mu)] < 0, \quad (17)$$

for any positive μ.

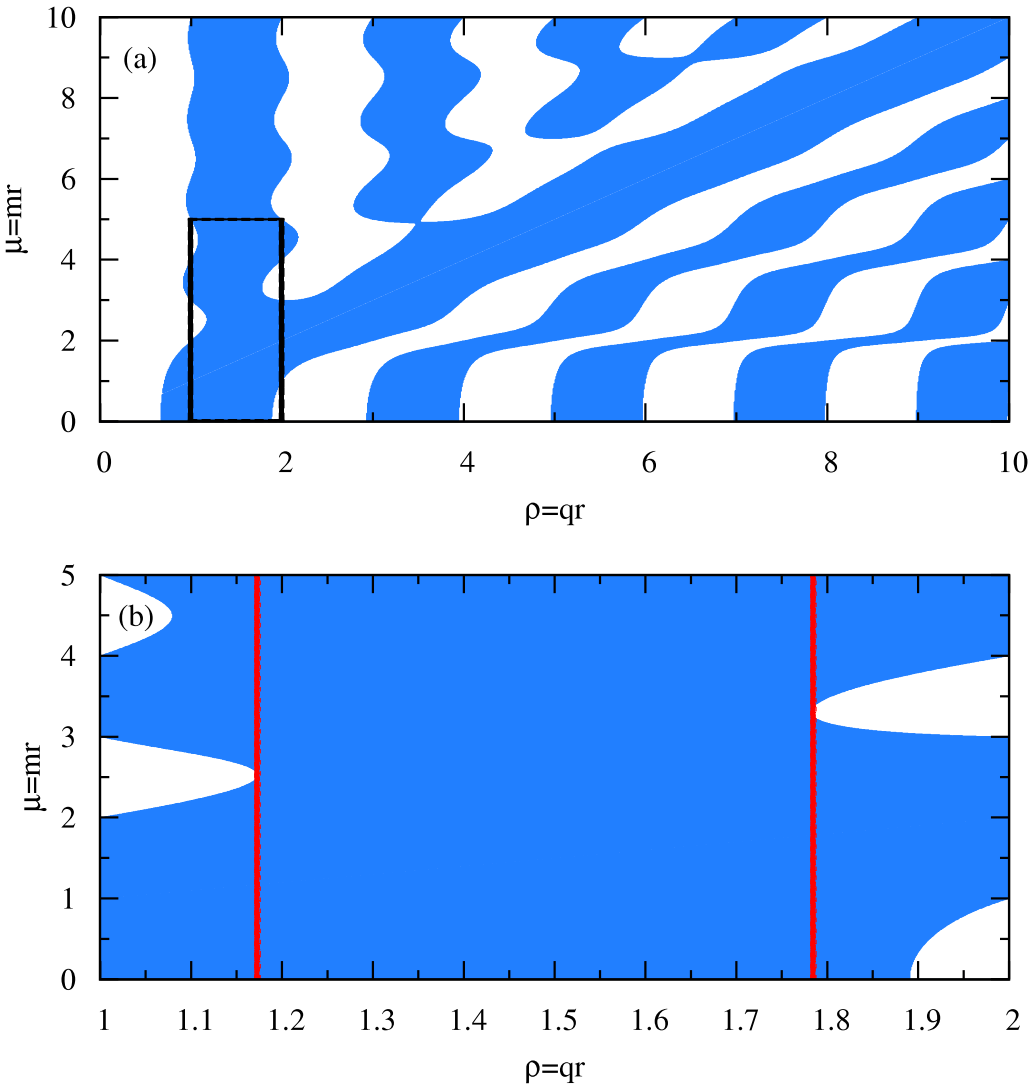

Figure 2: (Color online) a) Visualization of the sufficient condition $f(\rho, \mu) < 0$ given by (17) for the stability of q-twisted states for the model (9) ($N = \infty$). The condition is fulfilled in the blue region; b) enlargement of the rectangle in the region $1 < \rho < 2$, where red vertical lines bound the stability interval $\rho_1 < \rho < \rho_2$ given by Theorem 1.

In Fig. 2a the corresponding (ρ, μ) regions, where this inequality holds are shown with blue color. Note, that since in (17) we require function f to be negative for any positive real μ, this condition is more restrictive than (16). Let us now examine the set of values of parameter ρ where this conditions holds for all μ

a) If $s(\rho) > 0$, condition (17) cannot hold. Indeed, the following is true

$$\frac{1}{2}[|s(\rho+\mu)| + |s(\rho-\mu)|] < s(\rho)$$

for sufficiently large μ.

b) If $\rho > 2$ and $s(\rho) < 0$, condition (17) is also violated. Indeed, for $\mu = 2$

$$\begin{aligned} & s(\rho) - \frac{1}{2}[s(\rho+\mu) + s(\rho-\mu)] \\ & = \frac{\sin(\pi\rho)}{\pi\rho} - \frac{1}{2}\left[\frac{\sin(\pi\rho+2\pi)}{\pi\rho+2\pi} + \frac{\sin(\pi\rho-2\pi)}{\pi\rho-2\pi}\right] \\ & = \frac{\sin(\pi\rho)}{\pi}(\frac{1}{\rho} - \frac{1}{2}(\frac{1}{\rho+2} + \frac{1}{\rho-2})) = \frac{-4s(\rho)}{\rho^2-4} > 0. \end{aligned}$$

c) Therefore, the only possible parameter-ρ interval, where (17) can be satisfied is $1 < \rho < 2$. As it can be concluded from Fig. 2b the stability holds for all $\rho_1 < \rho < \rho_2$ where ρ_1 and ρ_2 are the roots of the system of transcendental equations

$$\begin{cases} f(\rho,\mu) = 0 \\ \dfrac{\partial f(\rho,\mu)}{\partial \mu} = 0 \end{cases} \tag{18}$$

in the intervals $2 < \mu < 3$ and $3 < \mu < 4$, respectively.

Theorem 1. *q-twisted state is a stable stationary solution of the model* (9)*,* (7) *if* $\rho_1 < \rho < \rho_2$*, where* $\rho_1 \approx 1.1787$ *and* $\rho_2 \approx 1.7829$ *are roots of Eq.s.* (18) *in the interval* $2 < \mu < 3$ *and* $3 < \mu < 4$ *respectively.*

In Fig. 2b the (ρ, μ)-parameter region of stability guaranteed by Theorem 1 is delimited by red lines.

Note that Theorem 1 is valid only for the spatially continuous version of Eq. (5) ($N = \infty$), but we expect it to hold for large N too. Numerical simulations show that this is true even for moderately large N.

In Fig. 3 the stable q-twisted states are marked by solid points, for the finite-dimensional system (5) of $N = 100$ oscillators and $0 < r < 1$, as obtained by direct numerical simulations. As one can observe these points fill, almost perfectly, the $N = \infty$ region provided by Theorem 1. In addition to the hyperbola-like stability region, there are other regions of stability of q-twisted states according to Fig. 3, as there are many others solid dots outside the red-bounded region. This is not in contradiction to Theorem 1 since the stability condition (17) is only sufficient but not necessary, and stable twisted states which do not satisfy this condition may exist for both infinite and finite N.

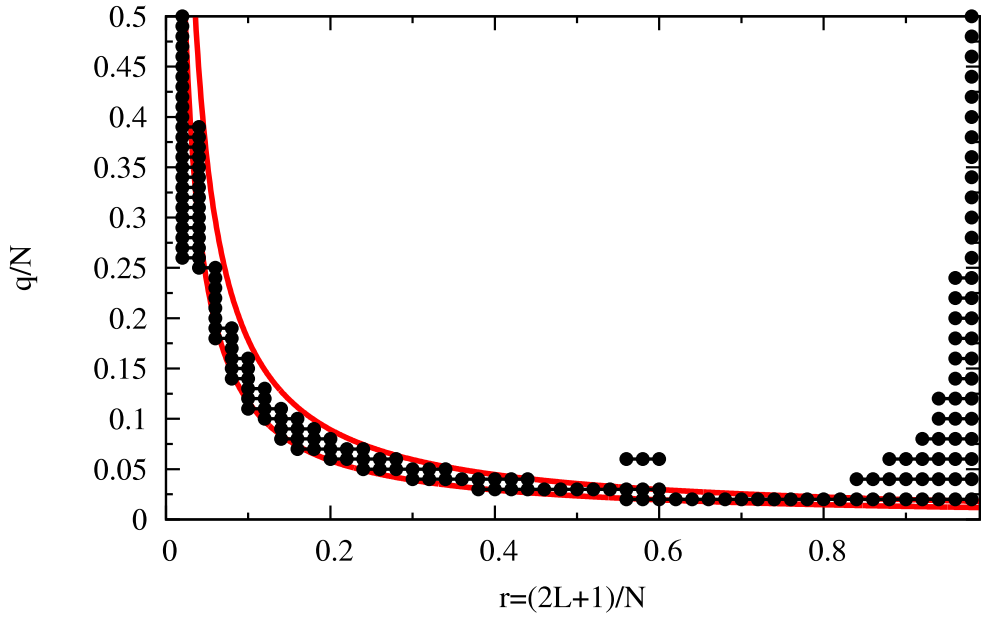

Figure 3: Stability of the q-twisted states of (5) for $N = 100$ (solid dots) obtained from direct numerical simulations. The hyperbola-like region, delimited by red lines, corresponds to the $\rho_1 < \rho < \rho_2$ stability interval given by Theorem 1.

Remark. The family of twisted states resulting from Theorem 1 was also obtained in [Tsimring *et al.*(2005)Tsimring, Rulkov, Larsen, and Gabbay]. However, the analysis was limited to numerical simulations and apparently the other stable twisted states were not detected.

Let us examine the existence of stable q-twisted states lying outside of the region given by Theorem 1. First, we determine the regions where these additional stable q-twisted states cannot exist. In fact, the previously made statement about absence of stable q-twisted states under the condition $s(qr) > 0$ remains valid when the values of μ are restricted to mr, where m is an integer. We can immediately obtain a few conclusions from this:

- 1-twisted state (standard splay state) can never be stable for $r < 1$;
- any q-twisted state is unstable for r in the interval $0 < r < 1/q$;
- any q-twisted state with odd q is unstable for r in the interval $\frac{q}{q+1} < r < 1$

Analyzing these statements and Fig. 2a we can expect the appearance of stable q-twisted states in the regions $3 < \rho < 4, 5 < \rho < 6, \ldots$ etc.. Additional regions of stability are found for infinite N by exploring systematically the corresponding (r, q)-parameter regions, see Fig. 4.

4 Stability analysis of the twisted states for finite N

In this section we prove, that if a twisted state if asymptotically stable under the infinite dimensional dynamics (9), then it is also asymptotically stable under the finite-dimensional dynamics (5) for sufficiently large N. Actually, we have to strengthen the stability conditions (16), as

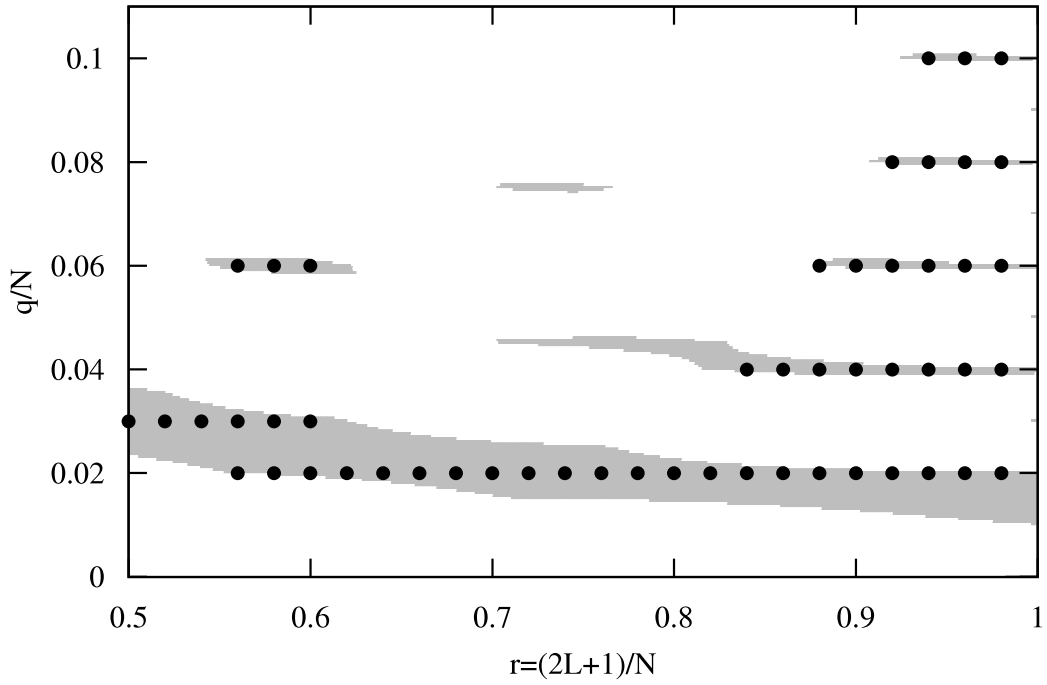

Figure 4: Stability of the q-twisted states of (5) for $N = 100$ (solid dots) obtained from numerical simulations. Conditions (16) are satisfied in shadowed regions with a 10^{-3} precision. Note, that all dots lies inside the shadowed region.

follows: There exists an $\alpha > 0$ such, that for all $m = 1, 2, 3, \ldots$ we have

$$s(qr) - \frac{1}{2}[s(qr + mr) + s(qr - mr)] \leq -\alpha. \tag{19}$$

We shall remark at the end of the section that this condition is almost always automatically satisfied when (16) holds.

Proposition 1. *Let $\phi(x) = qx$ be a twisted state of the infinite system for which* (19) *holds. Then any L_2-perturbation $\eta(x, 0)$ of qx decays exponentially fast, with exponential speed at least α under the linearized dynamics* (12) *of the infinite system. Specifically,*

$$\begin{aligned} \frac{d}{dt}\|\eta(\cdot, t)\|_2^2 = \frac{2}{2\pi} \iint_0^{2\pi} G(x - y)\cos(q(x - y)) \\ \times (\eta(y, t) - \eta(x, t))\eta(x, t)dxdy \leq -2\alpha\|\eta(\cdot, t)\|_2^2, \end{aligned} \tag{20}$$

where $\|\cdot\|_2$ is the L_2-norm for functions of x in $[0, 2\pi]$ defined as

$$\|g\|_2^2 = \frac{1}{2\pi}\int_0^{2\pi} |g(x)|^2 dx \tag{21}$$

and G is defined by (7)*.*

Proof. By Parseval's theorem

$$\|\eta(\cdot, t)\|_2^2 = \sum_{m=\infty}^{\infty} |\tilde{\eta}_m(t)|^2, \tag{22}$$

where the Fourier coefficients $\tilde{\eta}_m(t)$ satisfy (14). Hence, under condition (19),

$$\begin{aligned}\frac{d}{dt}|\tilde{\eta}_m(t)|^2 &= 2\left[\tilde{G}_q - \frac{1}{2}[\tilde{G}_{q+m} + \tilde{G}_{q-m}]\right]|\tilde{\eta}_m(t)|^2 \\ &= 2\left[s(qr) - \frac{1}{2}[s((q+m)r) + s((q-m)r)]\right]|\tilde{\eta}_m(t)|^2 \\ &\leq -2\alpha|\tilde{\eta}_m(t)|^2\end{aligned} \tag{23}$$

which implies (20). □

For finite N and the twisted state $\phi_i = \frac{2\pi qi}{N}$, $i = 1, \ldots, N$, the linearized system for a small perturbation, i. e.

$$\phi_i(t) = \frac{2\pi qi}{N} + \eta_i(t) \tag{24}$$

satisfies

$$\frac{d\eta_i}{dt} = -\frac{1}{2L+1}\sum_{j=i-L}^{i+L}\cos(\frac{2\pi q}{N}(i-j))(\eta_i(t) - \eta_j(t)) \tag{25}$$

and for the normalized Euclidian (l_2-)norm

$$\|\eta(t)\|_2^2 = \frac{1}{N}\sum_{i=1}^{N}|\eta_i(t)|^2 \tag{26}$$

we obtain

$$\frac{d}{dt}\|\eta(t)\|_2^2 = \frac{2}{(2L+1)N}\sum_{i=1}^{N}\sum_{j=i-L}^{i+L}\cos(\frac{2\pi q}{N}(i-j)) \times (\eta_j(t) - \eta_i(t))\eta_i(t). \tag{27}$$

In order to establish the precise connection between (27) and the corresponding expression in (20), we associate with a vector $v = (v_1, \ldots, v_N)$ the piece-wise constant function in $[0, 2\pi]$:

$$v^{(N)}(x) = v_i,\ if\ \frac{2\pi(i-\frac{1}{2})}{N} \leq x < \frac{2\pi(i+\frac{1}{2})}{N}\ (mod\ 2\pi). \tag{28}$$

Similarly, for matrices

$$w = \begin{pmatrix} w_{11} & \ldots & w_{1N} \\ \ldots & \ldots & \ldots \\ w_{N1} & \ldots & w_{NN} \end{pmatrix}$$

we define piece-wise constant function in $[0, 2\pi]^2$

$$\begin{aligned}w^{(N)}(x) = w_{ij},\ if\ \frac{2\pi(i-\frac{1}{2})}{N} \leq x \leq \frac{2\pi(i+\frac{1}{2})}{N}\ (\mathrm{mod}\ 2\pi) \\ \text{and}\ \frac{2\pi(j-\frac{1}{2})}{N} \leq y \leq \frac{2\pi(j+\frac{1}{2})}{N}\ (\mathrm{mod}\ 2\pi).\end{aligned} \tag{29}$$

It follows, that

$$\|v^{(N)}\|_2^2 = \frac{1}{2\pi}\int_0^{2\pi}|v^{(N)}(x)|^2dx = \frac{1}{2\pi}\cdot\frac{2\pi}{N}\sum_{i=1}^{N}v_i^2 = \|v\|_2^2 \tag{30}$$

and

$$\begin{aligned} \|w^{(N)}\|_2^2 &= \frac{1}{(2\pi)^2} \iint_0^{2\pi} |w^{(N)}(x,y)|^2 dxdy \\ &= \frac{1}{(2\pi)^2} \cdot (\frac{2\pi}{N})^2 \sum_{j=1}^{N} w_{ij}^2 = \|w\|_2^2. \end{aligned} \tag{31}$$

Furthermore, if the vector v depends on time, i.e. $v(t) = (v_1(t), \ldots, v_N(t))$, the corresponding piece-wise constant (in space) function becomes also time-dependent

$$\begin{aligned} v^{(N)}(x,t) &= v_i(t), \\ if\ \frac{2\pi(i-\frac{1}{2})}{N} &\leq x < \frac{2\pi(i+\frac{1}{2})}{N}\ (mod\ 2\pi). \end{aligned} \tag{32}$$

The partial derivative with respect to time becomes

$$\begin{aligned} \frac{\partial v^{(N)}}{\partial t}(x,t) &= \frac{dv_i(t)}{dt}, \\ if\ \frac{2\pi(i-\frac{1}{2})}{N} &\leq x < \frac{2\pi(i+\frac{1}{2})}{N}\ (mod\ 2\pi). \end{aligned} \tag{33}$$

If $v(t)$ satisfies the time evolution (5) of the finite system, we get

$$\begin{aligned} \frac{\partial v^{(N)}(x,t)}{\partial t} &= \frac{1}{2L+1} \sum_{j=-L}^{j=L} \sin\left(v_{i+j}(t) - v_i(t)\right), \\ if\ \frac{2\pi(i-\frac{1}{2})}{N} &\leq x < \frac{2\pi(i+\frac{1}{2})}{N}\ (mod\ 2\pi). \end{aligned} \tag{34}$$

We shall denote the right-hand side of (34) with $\frac{\partial^{(N)} v^{(N)}}{\partial t}$, whether or not this expression coincides with $\frac{\partial v^{(N)}(x,t)}{\partial t}$, i.e. whether or not $v^{(N)}(x,t)$ follows the finite system dynamics. Similarly, if $v^{(N)}(x,t)$ satisfies the time evoultion of the infinite system (9), we get

$$\frac{\partial v^{(N)}(x,t)}{\partial t} = -\int_0^{2\pi} G(x-y) \sin\left(v^{(N)}(y,t) - v^{(N)}(x,t)\right) dy \tag{35}$$

Again, we shall denote the right-hand side of (35) with $\frac{\partial^{(\infty)} v^{(N)}(x,t)}{\partial t}$, whether or not $v^{(N)}(x,t)$ follows the infinite system dynamics. Finally, we shall use

$$\frac{d^{(N)}}{dt} \|v^{(N)}(t)\|_2^2 = \frac{1}{\pi} \int_0^{2\pi} v^{(N)}(x,t) \frac{\partial^{(N)} v^{(N)}(x,t)}{\partial t} dx \tag{36}$$

and, similarly

$$\frac{d^{(\infty)}}{dt} \|v^{(N)}(t)\|_2^2 = \frac{1}{\pi} \int_0^{2\pi} v^{(N)}(x,t) \frac{\partial^{(\infty)} v^{(N)}(x,t)}{\partial t} dx. \tag{37}$$

We prove in the appendix

$$\begin{aligned}&\left|\frac{d^{(N)}}{dt}\|\eta^{(N)}(\cdot,t)\|_2^2-\frac{d^{(\infty)}}{dt}\|\eta^{(N)}(\cdot,t)\|_2^2\right|\\&\leq\frac{2}{\sqrt{N}}g(r,q,N)\|\eta^{(N)}(\cdot,t)\|_2^2,\end{aligned}\tag{38}$$

where

$$g(r,q,N)=\sqrt{(2\pi)^3\frac{q^2}{N}+\frac{\pi}{r}}+\frac{1}{\sqrt{N}}(2\pi q+\frac{1}{r}).\tag{39}$$

Note, that g is monotonically decreasing in N from $\frac{1}{2\pi}\left(\sqrt{(2\pi)^3q^2+\frac{\pi}{r}}+2\pi q+\frac{1}{r}\right)$ for $N=1$ to $\frac{1}{2\sqrt{\pi r}}$ for $N\to\infty$. If we combine this inequality with Proposition 1, we obtain the main theorem of this section.

Theorem 2. *Suppose, there exists $\alpha>0$ such that for all $m=1,2,3,\ldots$*

$$s(qr)-\frac{1}{2}(s(qr+mr)+s(qr-mr))\leq-\alpha,\tag{40}$$

where $r=\frac{2L+1}{N}$ and $s(x)=\frac{\sin(\pi x)}{\pi x}$. Then the q-twisted state $\phi_i=\frac{2\pi qi}{N}, i=1,\ldots,N$ of the finite system with parameters L,N is asymptotically stable, provided that

$$\frac{\sqrt{N}}{g(r,q,N)}>\frac{1}{\alpha},\tag{41}$$

where g is bounded and monotonically decreasing in N, given by (39)*.*

Proof. We prove that for any small perturbation $\eta(t)$ of the q-twisted state of the finite-dimensional system (24) we have

$$\frac{d}{dt}\|\eta(t)\|_2^2\leq-\epsilon\|\eta(t)\|_2^2\tag{42}$$

for some $\epsilon>0$ under the linearized finite-dimensional dynamics. Indeed,

$$\begin{aligned}&\frac{d}{dt}\|\eta(t)\|_2^2=\frac{d}{dt}^{(N)}\|\eta^{(N)}(\cdot,t)\|_2^2\leq\frac{d^{(\infty)}}{dt}\|\eta^{(N)}(\cdot,t)\|_2^2\\&+\left|\frac{d}{dt}^{(N)}\|\eta^{(N)}(\cdot,t)\|_2^2-\frac{d^{(\infty)}}{dt}\|\eta^{(N)}(\cdot,t)\|_2^2\right|\\&\leq-2\alpha\|\eta^{(N)}(\cdot,t)\|_2^2+\frac{2}{\sqrt{N}}g(r,q,N)\|\eta^{(N)}(\cdot,t)\|_2^2.\end{aligned}\tag{43}$$

The strict inequality (41) implies (42) which implies the asymptotic stability of the q-twisted state. □

Remark. The applicability of Theorem 2 depends essentially on condition (40). We now argue that in almost all cases this condition holds. Let us use the function f introduced in (17):

(a) If $\rho_1<qr<\rho_2$, where ρ_1,ρ_2 are given in Theorem 1, consider the function $f(qr,\mu)$ for fixed qr and $\mu\in[0,\infty]$. This function has a global maximum in the interval $\mu\in(2,3)$ or $\mu\in(3,4)$ or both. This maximum is necessarily negative and setting it to $-\alpha$ defines $\alpha>0$ which satisfies (40).

(b) The other asymptotically stable twisted states of the infinite dimensional system satisfy (40) without satisfying (17). Consider $f(qr, mr)$ for fixed q and r as a function of the discrete argument m. Fig. 2 suggests that this function also has a global maximum. Again, in this case, the maximum must be negative and we set it to $-\alpha$. The only exception would be the case where $f(qr, mr) \xrightarrow[m\to\infty]{} 0$.

Once (40) is satisfied for certain r, q, α and a minimum system size N is established through (41), the problem arises, that $L = \frac{Nr-1}{2}$ in general is not an integer. However, the maximum of $f(qr, \mu)$ as a function of μ, respectively $f(qr, mr)$ as a function of m depends smoothly on r. Therefore, choosing either the next lower (or the next higher) integer L will still satisfy (40) with the same α.

5 Comparison of analytical and numerical results

In previous Ch.s. 3, 4 we proposed some analytics about stability of the q-twisted states for the repulsive system Eq. (5) and for it continuous limit Eq. (9), and are able now to compare the rigorous results with numerical simulations. As direct numerical simulation approve, see Fig. 3, there are two main series of stable q-twisted states in the r, q-parameter plane of the model (5). But only twisted states from the parameter region, bounded with red lines, are captured by the sufficient conditions of Theorem 1, which is proven for the case of $N = \infty$. Moreover, the sufficient conditions here (red lines) seems to be also necessary for all $r < 1/2$. For the second region, as shown on Fig. 4 numerical experiments perfectly fits in conditions, given by Theorem 2, which are shown in light-gray color. Now one have an option to decide, whether to use continuous limit approach and sufficient conditions of Theorem 1 even for moderately large N and $L > 1$ or catch up with conditions, given by Theorem 2 which allows to verify stability for any number of oscillators N as well as for any range of coupling L.

6 Multi-twisted states

Detailed numerical simulations of the discrete model given by Eq. (5) reveal the existence of more complex stationary solutions - so called multi-twisted states. They are also equilibrium points of Eq. (5). While in the case of q-twisted states phase differences between neighboring oscillators remain constant (equal $2\pi q/N$), in the case of multi-twisted states they vary around the ring mostly approximating two opposite values: $2\pi q/N$ and $-2\pi q/N$. Typical examples of multi-twisted states are given in Fig. 5. As one can see, for each state there is a sector on the ring where phase differences between the neighboring oscillators are almost constant at, say, $2\pi q/N$, and another sector where they are almost constant at $-2\pi q/N$. Between these two sectors the phase differences make a transition from $2\pi q/N$ to $-2\pi q/N$ and vice versa. Interestingly, the graph of the transitions resembles the well-known Gibbs phenomenon for Fourier series.

We have detected the appearance of the multi-twisted states in the model (5) for different N and rather small $L = 2, 3..$, but never for the classical nearest-neighbor lattice with $L = 1$. Moreover, we have found that for some N and L the multi-twisted states have a rather large basin of attraction, or ßync basin"(in the terminology of [Wiley, Strogatz, and Girvan(2006)]).

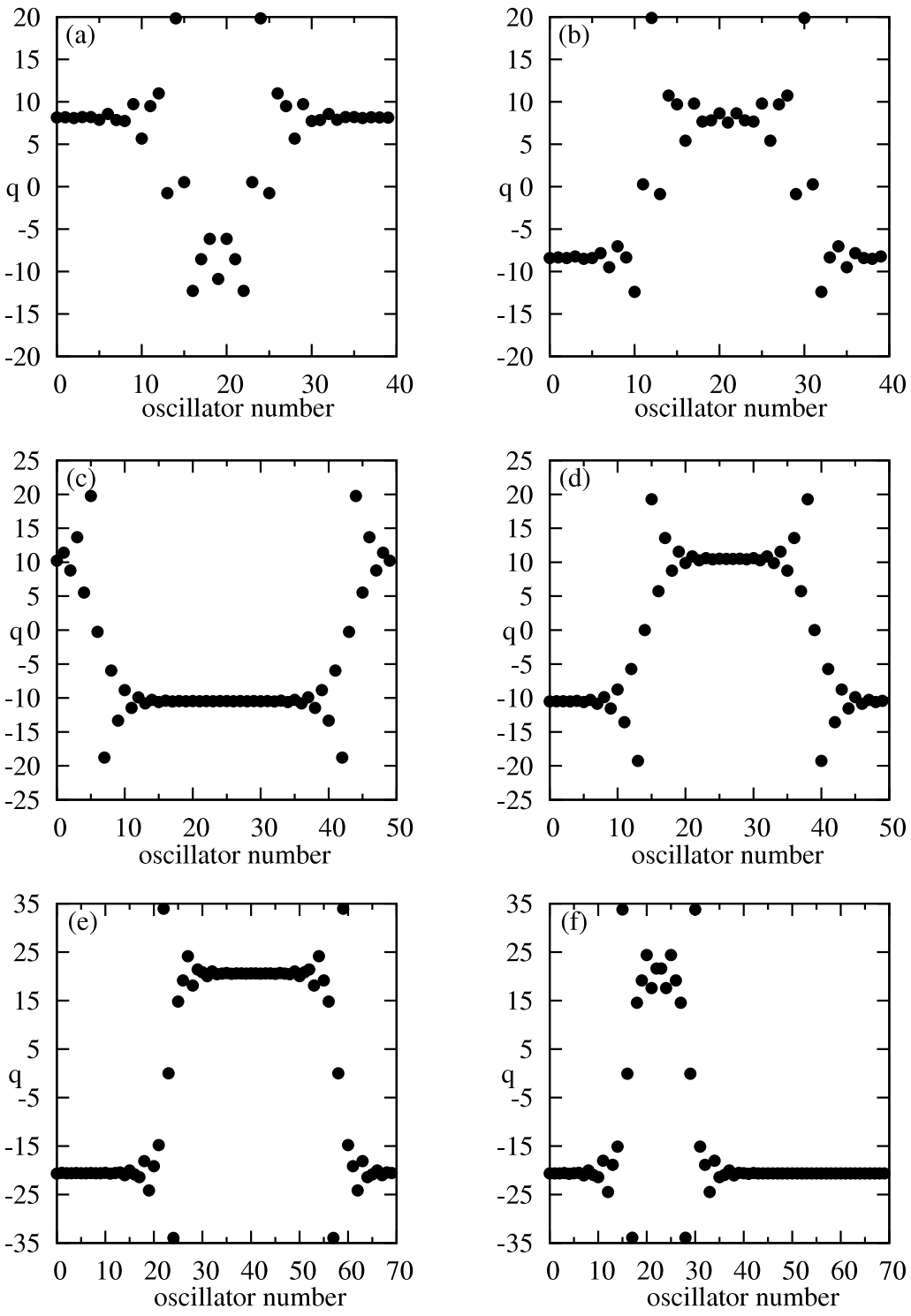

Figure 5: Examples of multi-twisted states for the repelling Kuramoto model (5). a-b) $N = 40, L = 3$; c-d) $N = 50, L = 2$; and e-f) $N = 70, L = 3$. Each multi-twisted state is a stable equilibrium point of (5) with the following property: The phase difference between neighboring oscillators is approximately $2\pi q/N$ in one sector of the ring, $-2\pi q/N$ in another sector, and it has intermediate values between the two sectors. Therefore, they provide the clock-wise and anti clock-wise rotations respectively. The multi-twisted states can be interpreted as periodic orbit of the period N, that are close to heteroclinic cycle, which represents heteroclinic oscillations in the respective translative dynamical system (translative means time is replaced by space variable i).

Indeed, e.g. for $N = 35$ and $L = 2$ our simulations from 10.000 randomly chosen initial conditions give rise only two types of multi-twisted (8.669 of 10.000) and q-twisted states with $q = \pm 9$ (21 of 10.000), $q = \pm 10$ (1220 of 10.000), $q = \pm 11$ (88 of 10.000), $q = \pm 12$ (2 of 10.000).

The examples presented in Fig. 5, demonstrate that multi-twisted states are distinguished from each other by the number and length of the clock-wise and anti-clock-wise intervals. As it is suggested by our numerical simulations, the number of different multi-twisted states grows with N and the transitions between the intervals become sharper. At the same time, the lengths of the clock-wise and anti-clock-wise intervals are bounded from below if N is fixed, but they can tend to zero with increasing N. E.g., we have detected only two distinct multi-twisted states for $N = 40$ (up to a constant phase shift of all oscillators), Fig. 5 c, d, four such states for $N = 70$, two of them presented in Fig. 5 e, f, and already more than a dozen of them for $N = 100$. More extensive numerical simulations show that the number of different stable multi-twisted states grows exponentially with N giving rise, due to this, to the phenomenon of spatial chaos [Jensen(1985), Coullet, Elphick, and Repaux(1987), Chow and Mallet-Paret(1995), Nizhnik, Nizhnik, and Hasler(2002), Afraimovich(2005), Fernandez, Luna, and Ugalde(2009)] in the repulsive network given by Eq. (3). On the other hand, the number of different q-twisted states in Kuramoto model (1) grows only linearly with N, and there are no stable multi-twisted states, as analyzed in [Wiley, Strogatz, and Girvan(2006)]. Hence, the repulsive Kuramoto network (3) has a much more complex internal multistable structure of spatio-temporal patterns. We leave a more detailed analysis of this issue for a future study.

7 Acknowledgments

The authors thank M. Wolfrum, B. Fiedler and A. Pikovskiy for illuminating discussions. T. Girnyk and Yu. Maistrenko thank the Laboratory of Nonlinear Systems, EPFL for hospitality during their stay there.

8 Appendix

Here, we prove the inequality (38). We can rewrite (27) as

$$\frac{d}{dt}\|\eta(t)\|_2^2 = \frac{4\pi}{N^2}\sum_{i,j=1}^{N} G_{ij}C_{ij}(\eta_j(t) - \eta_i(t)), \tag{44}$$

where

$$G_{ij} = \begin{cases} \frac{1}{2\pi r},\ |i-j| \le L,\ r = \frac{2L+1}{N} \\ 0,\ |i-j| > L \end{cases} \tag{45}$$

and

$$C_{ij} = \cos\left(\frac{2\pi q}{N}(i-j)\right). \tag{46}$$

Using (28) and (29) we can write

$$\frac{d^{(N)}}{dt}\|\eta^{(N)}(t)\|_2^2 = \frac{2}{(2\pi)}\iint_0^{2\pi} G^{(N)}(x,y)C^{(N)}(x,y) \times (\eta^{(N)}(y,t) - \eta^{(N)}(x,t))\eta^N(x,t)dxdy. \quad (47)$$

Therefore, using (30)

$$\begin{aligned}
&\left|\frac{d^{(N)}}{dt}\|\eta^{(N)}(\cdot,t)\|_2^2 - \frac{d^{(\infty)}}{dt}\|\eta^{(N)}(\cdot,t)\|_2^2\right| \\
&= |\frac{2}{2\pi}\iint_0^{2\pi} \left[G^{(N)}(x,y)C^{(N)}(x,y) - G(x,y)\cos\left(q(x-y)\right)\right] \\
&\times \left(\eta^{(N)}(y,t) - \eta^{(N)}(x,t)\right)\eta^{(N)}(x,t)dxdy| \\
&\leq \frac{2}{2\pi}\iint_0^{2\pi} \left|G^{(N)}(x,y)C^{(N)}(x,y) - G(x,y)\cos\left(q(x-y)\right)\right| \cdot \\
&\times |\eta^{(N)}(y,t)||\eta^{(N)}(x,t)|dxdy \\
&+ \frac{2}{2\pi}\iint_0^{2\pi} \left|G^{(N)}(x,y)C^{(N)}(x,y) - G(x,y)\cos\left(q(x-y)\right)\right| \\
&\times |\eta^{(N)}(y,t)|^2 dxdy = T_1 + T_2
\end{aligned} \quad (48)$$

Applying the Cauchy-Schwarz inequality to the first term, we obtain

$$T_1 \leq 2\sqrt{\iint_0^{2\pi} \left|G^{(N)}C^{(N)} - G\cos\left(q(x-y)\right)\right|^2 dxdy} \times \|\eta^{(N)}(\cdot,t)\|_2^2 \quad (49)$$

and the second term can be bounded as follows

$$T_2 \leq 2\sup_y \int_0^{2\pi} |G^{(N)}(x,y)C^{(N)}(x,y) - G(x,y)\cos\left(q(x-y)\right)|dx\|\eta^{(N)}(\cdot,t)\|_2^2. \quad (50)$$

The functions G and $G^{(N)}$ limit the 2-dimensional integration domain. Let

$$\begin{aligned}
S &= \left\{(x,y) \in [0,2\pi]^2 \mid G(x-y) \neq 0\right\} \\
S^{(N)} &= \left\{(x,y) \in [0,2\pi]^2 \mid G^{(N)}(x,y) \neq 0\right\}.
\end{aligned} \quad (51)$$

The domain $S^{(N)}$ is shaded in Fig. 6, whereas S is the domain enclosed by the line $x - y =$

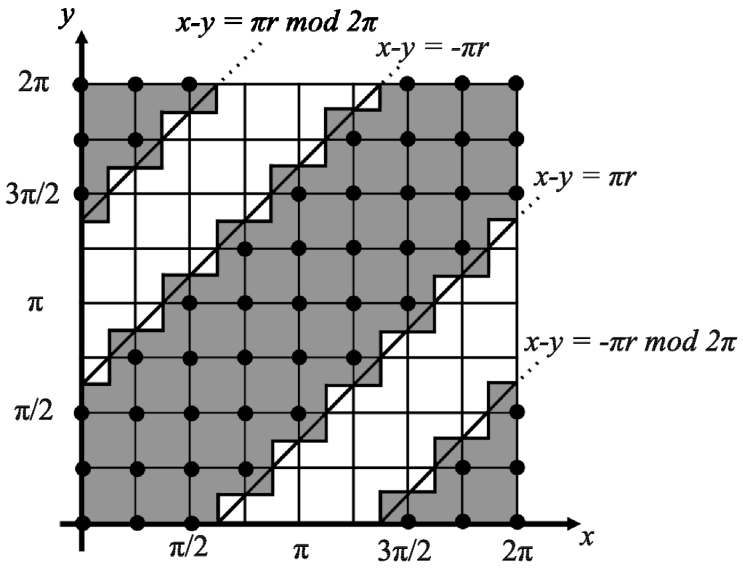

Figure 6: Domains $S^{(N)}$ (shaded) and S (between the lines $x - y = \pi r \ mod \ 2\pi$). $N = 8$, $L = 2$, $r = \frac{2L+1}{N} = \frac{5}{8}$

$\pi r \mod 2\pi$ and $x - y = -\pi r \mod 2\pi$. The integrals in (49) and (50) are bounded in two parts, namely on $S \cap S^{(N)}$ and on $(S \backslash S^{(N)}) \cup (S^{(N)} \backslash S)$:

$$\begin{aligned}
&\iint_0^{2\pi} \left| G^{(N)}(x,y)C^{(N)}(x,y) - G(x-y)\cos\left(q(x-y)\right)\right|^2 dxdy \\
&\frac{1}{2\pi r} \iint_{S \cap S^N} \sup_{x,y} \left| C^{(N)}(x,y) - \cos\left(q(x-y)\right)\right|^2 dxdy \\
&+ \frac{1}{2\pi r} \iint_{S^{(N)} \backslash S} \sup_{x,y} \left| C^{(N)}(x,y)\right|^2 dxdy \\
&+ \frac{1}{2\pi r} \iint_{S \backslash S^{(N)}} \sup_{x,y} \left|\cos\left(q(x-y)\right)\right|^2 dxdy.
\end{aligned} \tag{52}$$

$C^{(N)}(x,y)$ and $\cos\left(q(x-y)\right)$ have identical values at the grid points $\left(\frac{2\pi i}{N}, \frac{2\pi j}{N}\right)$, $C^{(N)}$ is constant in a square of side length $\frac{2\pi}{N}$ around the grid points, and the partial derivatives of $\cos\left(q(x-y)\right))$ are bounded by q. Hence

$$\left| C^{(N)}(x,y) - \cos\left(q(x-y)\right)\right| \leq \frac{2\pi q}{N}, \forall\, (x,y) \in [0,2\pi]^2. \tag{53}$$

Furthermore, $C^{(N)}(x,y)$ being the value of a cosine is bounded by 1. Therefore

$$\begin{aligned}
&\iint_0^{2\pi} \left|G^{(N)}(x,y)C^{(N)}(x,y) - G(x-y)\cos\left(q(x-y)\right)\right|^2 dxdy \\
&\leq \frac{1}{2\pi r}\left(\frac{4\pi^2 q^2}{N^2}|S| + |S^{(N)}\backslash S| + |S\backslash S^{(N)}|\right) \\
&= \frac{1}{2\pi r}\left(\frac{4\pi^2 q^2}{N^2}4\pi^2 r + \frac{\pi^2 N}{N^2} + \frac{\pi^2 N}{N^2}\right) = \frac{(2\pi)^3 q^2}{N^2} + \frac{\pi}{Nr}.
\end{aligned} \tag{54}$$

Similarly,

$$\begin{aligned}
&\sup_y \int_0^{2\pi} \left|G^{(N)}(x,y)C^{(N)}(x,y) - G(x-y)\cos\left(q(x-y)\right)\right| dx \\
&\leq \frac{1}{2\pi r}\sup_y \int_{[S\cap S^{(N)}]_y} \left|C^{(N)}(x,y) - \cos\left(q(x-y)\right)\right| dx \\
&+ \frac{1}{2\pi r}\sup_y \int_{[S^{(N)}\backslash S]_y} \left|C^{(N)}(x,y)\right| dx \\
&+ \frac{1}{2\pi r}\sup_y \int_{[S\backslash S^{(N)}]_y} \left|\cos\left(q(x-y)\right)\right| dx,
\end{aligned} \tag{55}$$

where $[A]_y = \{x|(x,y) \in A\}$ for any set A in $[0,2\pi]^2$ Hence,

$$\begin{aligned}
&\int_0^{2\pi} \left|G^{(N)}(x,y)C^{(N)}(x,y) - G(x-y)\cos\left(q(x-y)\right)\right| dx \\
&\leq \frac{1}{2\pi r}\left(\frac{2\pi q}{N}|[S\cap S^{(N)}]_y| + |[S^{(N)}\backslash S]_y| + |[S\backslash S^{(N)}]_y|\right) \\
&= \frac{1}{2\pi r}\left(\frac{2\pi q}{N}2\pi r + \frac{\pi}{N} + \frac{\pi}{N}\right) = \frac{2\pi q}{N} + \frac{1}{Nr}.
\end{aligned} \tag{56}$$

Combining all inequalities, we obtain

$$\begin{aligned}
&\left|\frac{d^{(N)}}{dt}\|\eta^{(N)}(\cdot,t)\|_2^2 - \frac{d^{(\infty)}}{dt}\|\eta^{(N)}(\cdot,t)\|_2^2\right| \\
&\leq 2\left(\sqrt{(2\pi)^3\frac{q^2}{N^2} + \frac{\pi}{Nr}} + \frac{2\pi q}{N} + \frac{1}{Nr}\right)\|\eta^{(N)}(\cdot,t)\|_2^2 \\
&= \frac{2}{\sqrt{N}}\left(\sqrt{(2\pi)^3\frac{q^2}{N} + \frac{\pi}{r}} + (2\pi q + \frac{1}{r})\frac{1}{\sqrt{N}}\right)\|\eta^{(N)}(\cdot,t)\|_2^2.
\end{aligned} \tag{57}$$

References

[Wiley, Strogatz, and Girvan(2006)] D. A. Wiley, S. H. Strogatz, and M. Girvan, “The size of the sync basin,” \bibfield journal \bibinfo journal Chaos\ \textbf \bibinfo volume 16,\ \bibinfo pages 015103, 8 (\bibinfo year 2006).

[Afraimovich *et al.*(1992)Afraimovich, Ezersky, Rainovich, Shereshevsky, and Zheleznyak] V. S. Afraimovich, A. B. Ezersky, M. I. Rainovich, M. A. Shereshevsky, and A. L. Zheleznyak, “Dynamical description of spatial disorder,” Physica D , 331–338 (1992).

[Shen(1996)] W. Shen, “Lifted lattices, hyperbolic structures, and topological disorders in coupled map lattices,” SIAM J. Appl. Math. **56**, 1379–1399 (1996).

[Degallier and Ijspeert(2010)] S. Degallier and A. Ijspeert, “Modelling discrete and rhythmic movements through motor primitives, a review,” Biol. Cybern. **103**, 319–338 (2010).

[Winfree(1967)] A. T. Winfree, J. Theoret. Biol **16** (1967).

[Winfree(2001)] A. T. Winfree, *The geometry of biological time*, 2nd ed., Interdisciplinary Applied Mathematics, Vol. 12 (Springer-Verlag, New York, 2001) pp. xxvi+777.

[Kuramoto(2002)] Y. Kuramoto, “Lecture notes in physics,” in *Interantional Sumposium on Mathematical Problems in Theoretical Physics*, Vol. 5 (Springer, Berlin, 2002).

[Kuramoto(1984)] Y. Kuramoto, *Chemical oscillations, waves, and turbulence*, Springer Series in Synergetics, Vol. 19 (Springer-Verlag, Berlin, 1984) pp. viii+156.

[Kopell and Ermentrout(1990)] N. Kopell and G. B. Ermentrout, “Phase transitions and other phenomena in chains of coupled oscillators,” \bibfield journal \bibinfo journal SIAM J. Appl. Math.\ \textbf \bibinfo volume 50,\ \bibinfo pages 1014–1052 (\bibinfo year 1990).

[Ermentrout(1985a)] G. B. Ermentrout, “The behavior of rings of coupled oscillators,” J. Math. Biol. **23**, 55–74 (1985a).

[Ermentrout and Kopell(1984)] G. B. Ermentrout and N. Kopell, “Frequency plateaus in a chain of weakly coupled oscillators. I,” \bibfield journal \bibinfo journal SIAM J. Math. Anal.\ \textbf \bibinfo volume 15,\ \bibinfo pages 215–237 (\bibinfo year 1984).

[Strogatz(2oo1)] S. H. Strogatz, “Exploring complex networks,” Nature , 268–276 (2oo1).

[Strogatz(1999)] S. H. Strogatz, “Collective dynamics of small-world networks,” Nature , 440–442 (1999).

[Boccaletti(2008)] S. Boccaletti, *The synchronized dynamics of complex systems*, Monograph Series on Nonlinear Science and Complexity, Vol. 6 (Elsevier B. V., Amsterdam, 2008) pp. xiv+243.

[Ermentrout(1985b)] G. B. Ermentrout, “Synchronization in a pool of mutually coupled oscillators with random frequencies,” \bibfield journal \bibinfo journal J. Math. Biol.\ \textbf \bibinfo volume 22,\ \bibinfo pages 1–9 (\bibinfo year 1985\natexlabb).

[Strogatz(2000)] S. H. Strogatz, “From Kuramoto to Crawford: exploring the onset of synchronization in populations of coupled oscillators,” \bibfield journal \bibinfo journal Phys. D\ \textbf \bibinfo volume 143,\ \bibinfo pages 1–20 (\bibinfo year 2000), bifurcations, patterns and symmetry.

[Mirollo and Strogatz(1990)] R. E. Mirollo and S. H. Strogatz, “Amplitude death in an array of limit-cycle oscillators,” J. Statist. Phys. **60**, 245–262 (1990).

[Daido(1997)] H. Daido, “Order function theory of macroscopic phase-locking in globally and weakly coupled limit-cycle oscillators,” Int. J. Bifurcation Chaos **7** (1997).

[Crawford and Davies(1999)] J. D. Crawford and K. T. R. Davies, “Synchronization of globally coupled phase oscillators: singularities and scaling for general couplings,” \bibfield journal \bibinfo journal Phys. D\ \textbf \bibinfo volume 125,\ \bibinfo pages 1–46 (\bibinfo year 1999).

[Ott *et al.*(2002)Ott, So, Barreto, and Antonsen] E. Ott, P. So, E. Barreto, and T. Antonsen, “The onset of synchronization in systems of globally coupled chaotic and periodic oscillators,” \bibfield journal \bibinfo journal Phys. D\ \textbf \bibinfo volume 173,\ \bibinfo pages 29–51 (\bibinfo year 2002).

[Ott and Antonsen(2008)] E. Ott and T. M. Antonsen, “Low dimensional behavior of large systems of globally coupled oscillators,” \bibfield journal \bibinfo journal Chaos\ \textbf \bibinfo volume 18,\ \bibinfo pages 037113, 6 (\bibinfo year 2008).

[Watanabe and Strogatz(1993)] S. Watanabe and S. H. Strogatz, “Integrability of a globally coupled oscillator array,” \bibfield journal \bibinfo journal Phys. Rev. Lett.\ \textbf \bibinfo volume 70,\ \bibinfo pages 2391–2394 (\bibinfo year 1993).

[Pikovsky and Rosenblum(2009)] A. Pikovsky and M. Rosenblum, “Self-organized partially synchronous dynamics in populations of nonlinearly coupled oscillators,” \bibfield journal \bibinfo journal Phys. D\ \textbf \bibinfo volume 238,\ \bibinfo pages 27–37 (\bibinfo year 2009).

[Kopell, Zhang, and Ermentrout(1990)] N. Kopell, W. Zhang, and G. B. Ermentrout, “Multiple coupling in chains of oscillators,” \bibfield journal \bibinfo journal SIAM J. Math. Anal.\ \textbf \bibinfo volume 21,\ \bibinfo pages 935–953 (\bibinfo year 1990).

[Kiem *et al.*(2004)Kiem, Ko, Jeong, and Moon] P.-J. Kiem, T.-W. Ko, H. Jeong, and H.-T. Moon, “Pattern formation in a two-dimensional array of oscillators with phase-shifted coupling,” Phys. Rev. E. **70**, 065–201 (2004).

[Lefort *et al.*(2009)Lefort, Tomm, Sarria, and Petersen] S. Lefort, C. Tomm, J.-C. Sarria, and C. C. Petersen, “The excitatory neuronal network of the c2 barrel column in mouse primary somatosensory cortex,” Neuron **61**, 301–316 (2009).

[Kuramoto and Battogtokh(2002)] Y. Kuramoto and D. Battogtokh, “Nonlinear phenomena in complex systems,” (2002).

[Abrams and Strogatz(2004)] D. M. Abrams and S. H. Strogatz, Phys. Rev. Lett. **93** (2004).

[Laing(2009)] C. R. Laing, “The dynamics of chimera states in heterogeneous Kuramoto networks,” \bibfield journal \bibinfo journal Phys. D\ \textbf \bibinfo volume 238,\ \bibinfo pages 1569–1588 (\bibinfo year 2009).

[Omelchenko, Wolfrum, and Maistrenko(2010)] O. E. Omelchenko, M. Wolfrum, and Y. L. Maistrenko, “Chimera states as chaotic spatio-temporal patterns,” Phys. Rev. E. **81** (2010).

[Jensen(1985)] M. H. Jensen, “Spatial chaos,” Physica Scripta **9**, 64–69 (1985).

[Coullet, Elphick, and Repaux(1987)] P. Coullet, C. Elphick, and D. Repaux, “Nature of spatial chaos,” Phys Rev. Lett. **58**, 431–434 (1987).

[Chow and Mallet-Paret(1995)] S.-N. Chow and J. Mallet-Paret, “Pattern formation and spatial chaos in lattice dynamical systems. I, II,” \bibfield journal \bibinfo journal IEEE Trans. Circuits Systems I Fund. Theory Appl.\ \textbf \bibinfo volume 42,\ \bibinfo pages 746–751, 752–756 (\bibinfo year 1995).

[Nizhnik, Nizhnik, and Hasler(2002)] L. P. Nizhnik, I. L. Nizhnik, and M. Hasler, “Stable stationary solutions in reaction-diffusion systems consisting of a 1-D array of bistable cells,” \bibfield journal \bibinfo journal Internat. J. Bifur. Chaos Appl. Sci. Engrg.\ \textbf \bibinfo volume 12,\ \bibinfo pages 261–279 (\bibinfo year 2002).

[Afraimovich(2005)] V. Afraimovich, “Some topological properties of lattice dynamical systems,” in \emph \bibinfo booktitle Dynamics of coupled map lattices and of related spatially extended systems, Lecture Notes in Phys., Vol. 671 (Springer, Berlin, 2005) pp. 153–179.

[Fernandez, Luna, and Ugalde(2009)] B. Fernandez, B. Luna, and E. Ugalde, “Spatial chaos of traveling waves has a given velocity,” Phys Rev. Lett. **80** (2009).

[Tsimring *et al.*(2005)Tsimring, Rulkov, Larsen, and Gabbay] L. S. Tsimring, N. F. Rulkov, M. L. Larsen, and M. Gabbay, “Repulsive synchronization in an array of phase oscillators,” Phys. Rev. E. **95**, 014–101 (2005).